Thermo X https://doi.org/10.70401/tx.2026.0011

Supplementary information

Poly(ionic liquid) thermal gels enabling compliant and adhesive interfaces for chip-scale thermal management

Jianhui Zeng, Taoying Rao, Hang Shi, Yilan Guo, Zhengwu Peng, Liejun Li, Rong Sun1, Yimin Yao

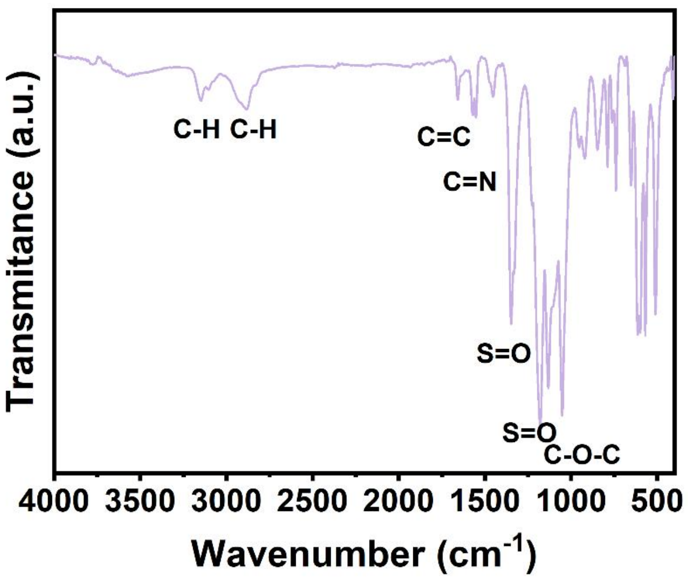

Figure S1. Infrared spectrum of VIm-3EO NTf_2.

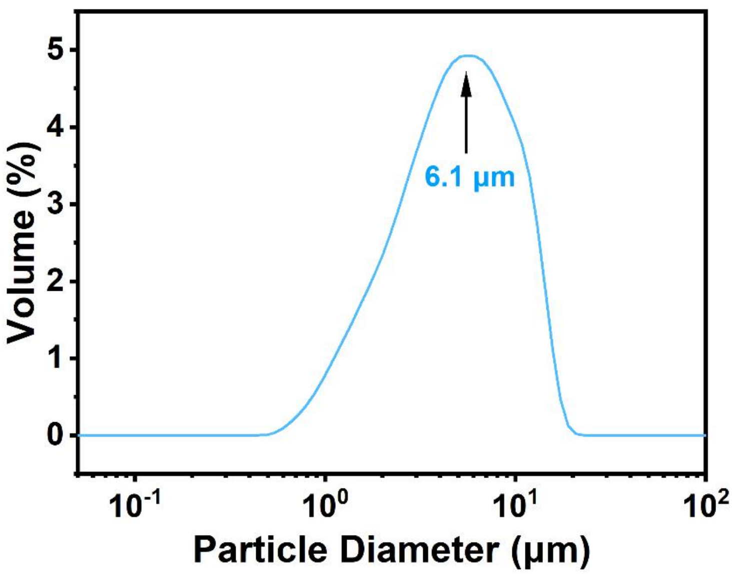

Figure S2. The proportion of particle size distribution of Al_2O_3.

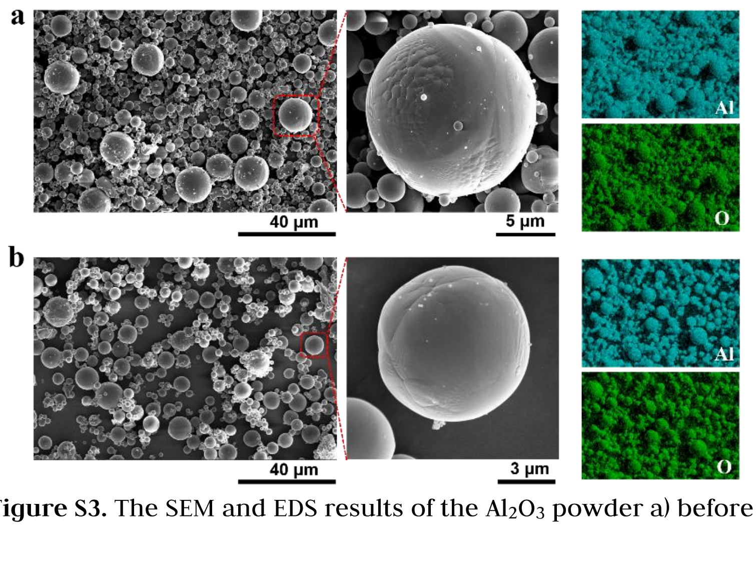

Figure S3. The SEM and EDS results of the Al_2O_3 powder a) before and b) after modification.

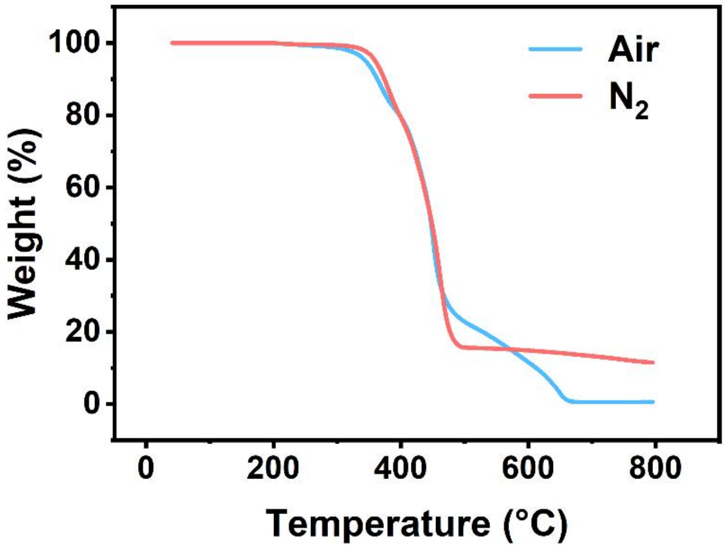

Figure S4. Thermogravimetric curve of ionic liquid monomer.

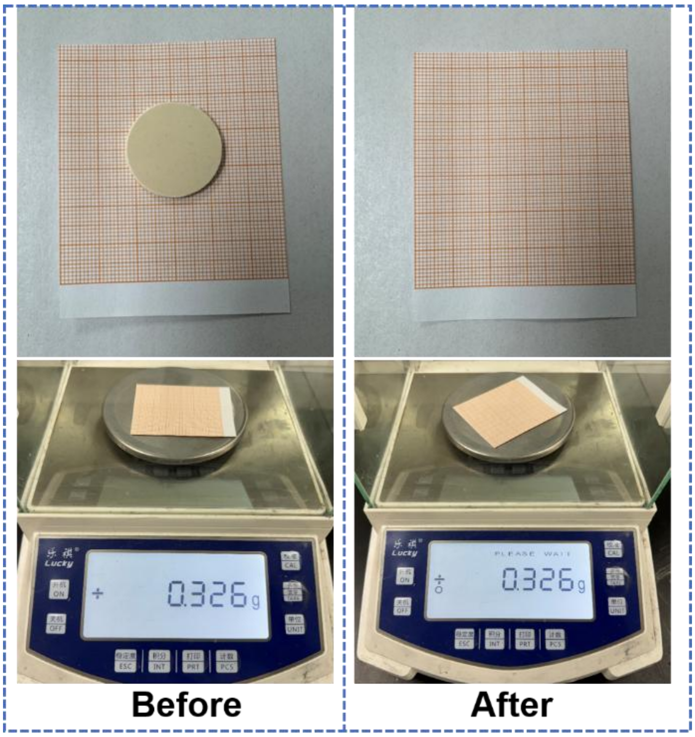

Figure S5. Optical images before and after the leakage test of 70 vol% conductive gel (85 °C， 24 h).

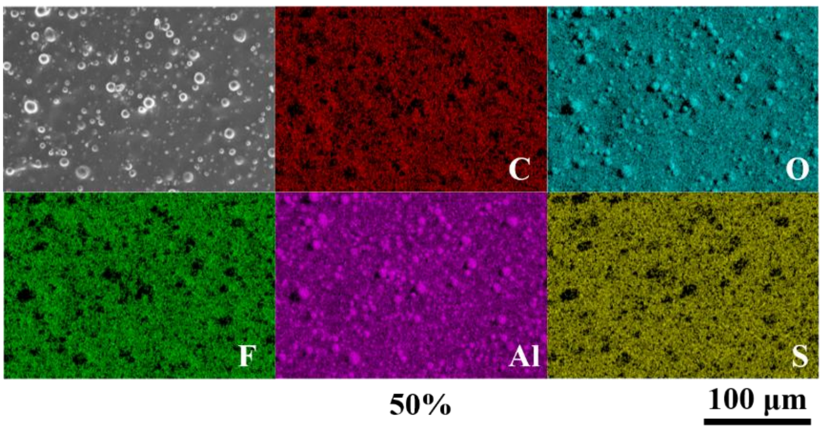

Figure S6. The EDS results of the 50% volume composites.

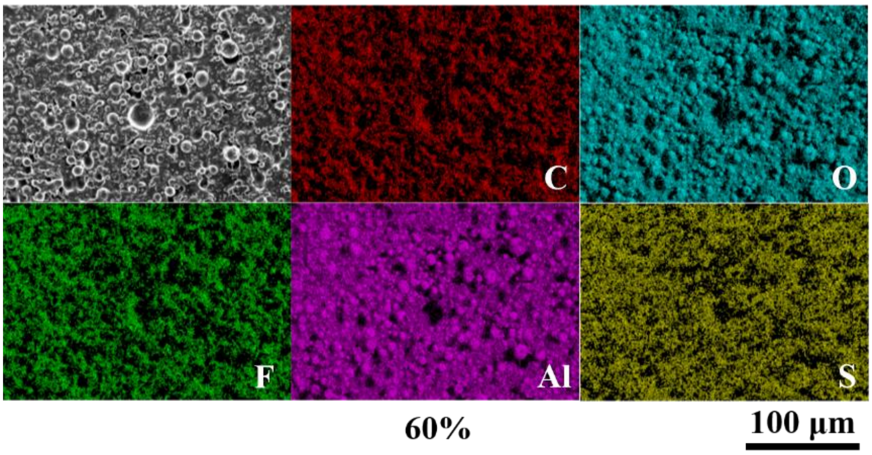

Figure S7. The EDS results of the 60% volume composites.

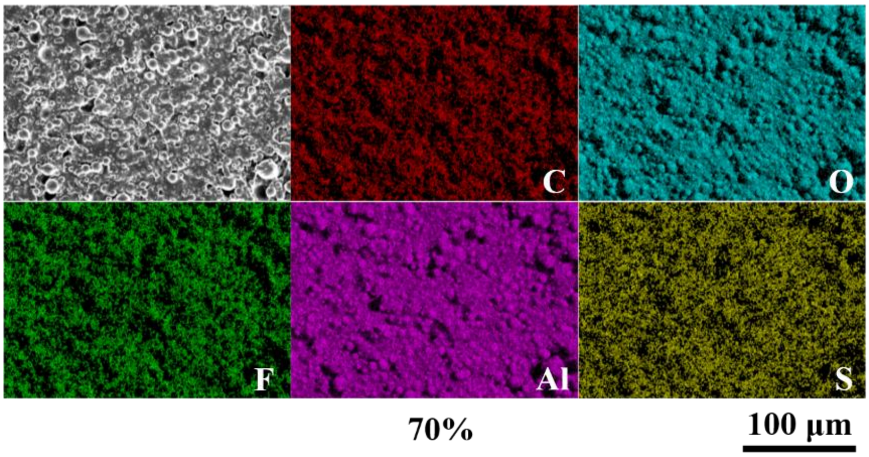

Figure S8. The EDS results of the 70% volume composites.

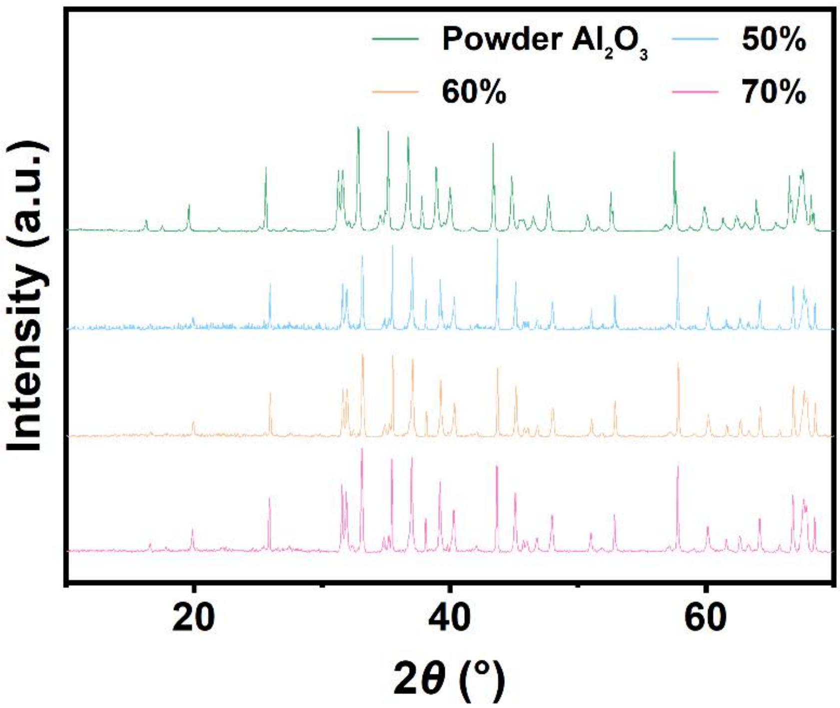

Figure S9. The XRD results of the Al_2O_3 and varying volume composites.

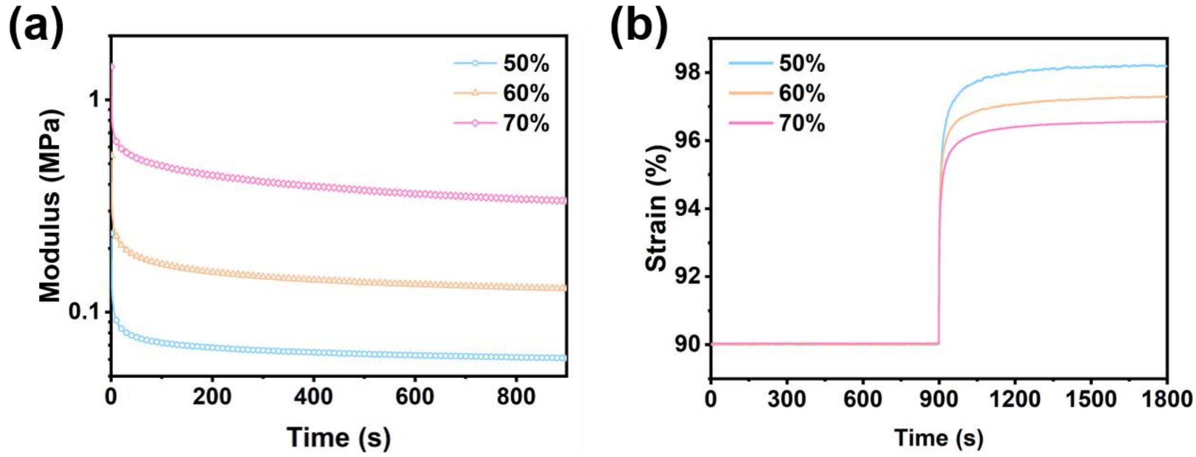

Figure S10. (a) The modulus of the composites at different volume fractions before stress relaxation for 15 minutes; (b) The rebound situation after 15 minutes of stress relaxation.

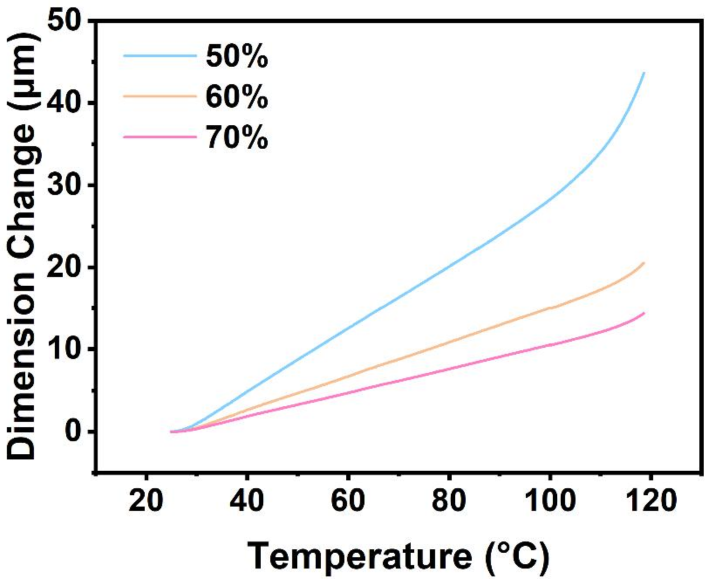

Figure S11. The CTE curves of composites with different filler contents

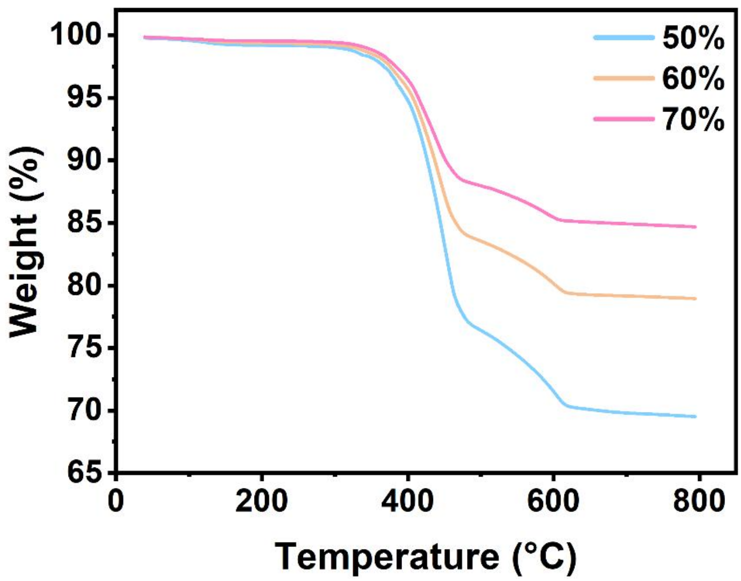

Figure S12. Thermogravimetric curves of composites under air atmosphere.

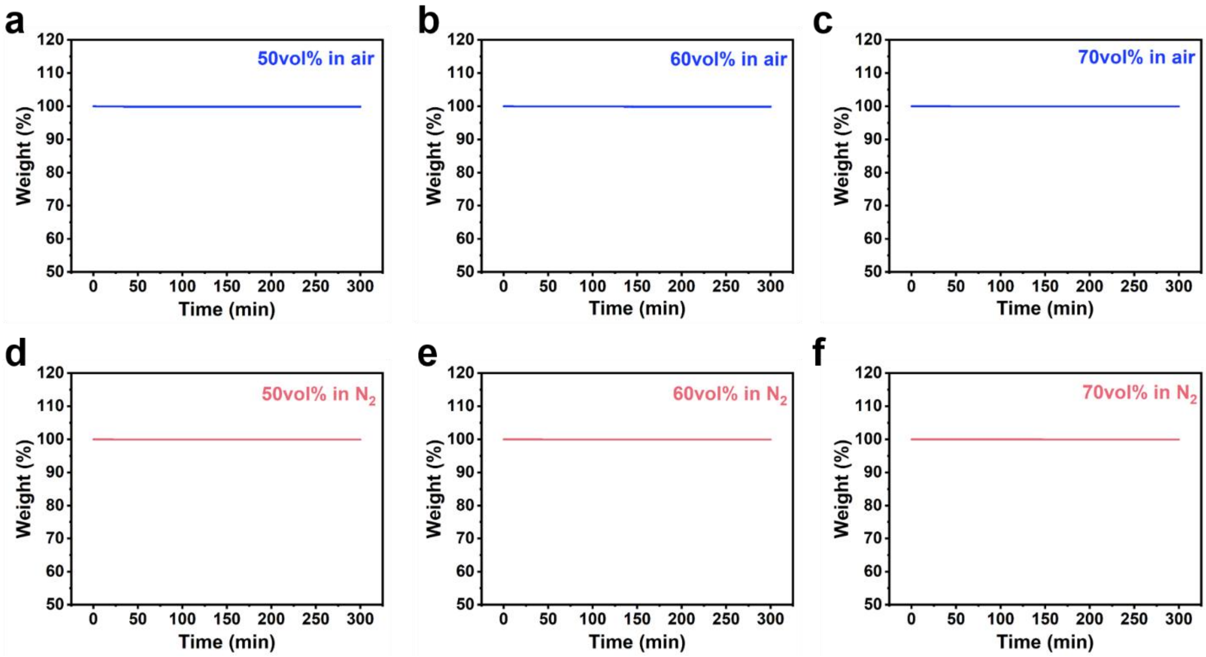

Figure S13. Thermogravimetric curves of composite materials with different volume fractions when they are heated at 150 °C for 300 minutes in air and N_2 atmospheres.

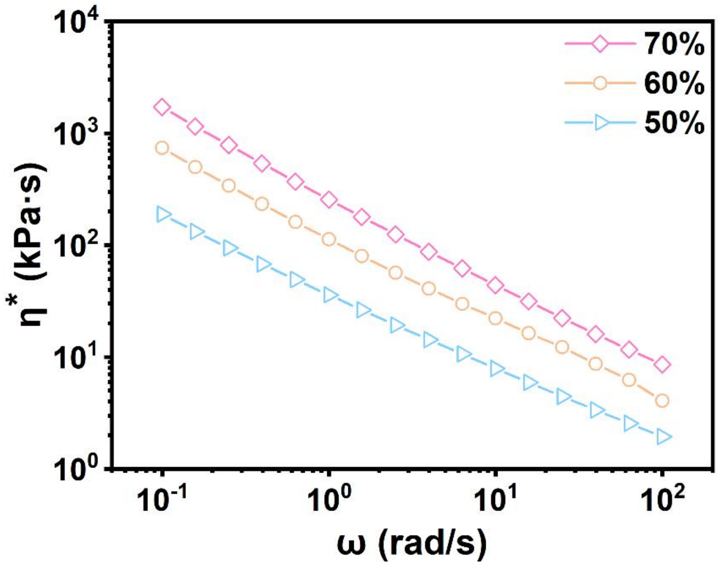

Figure S14. The complex viscosity of composites with different volume fractions.

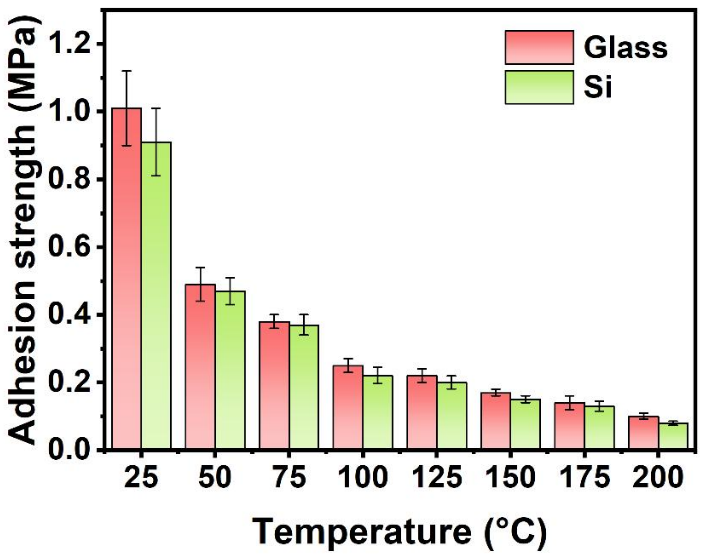

Figure S15. Adhesion strengths of 70 vol% composite to glass and silicon substrates at different temperatures.

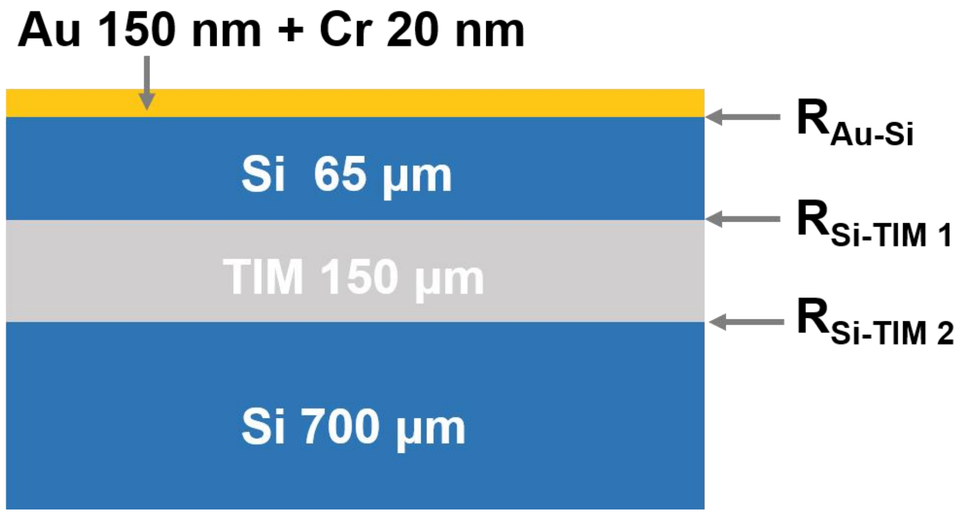

Figure S16. Schematic diagram of the sample structure for the FDTR test.

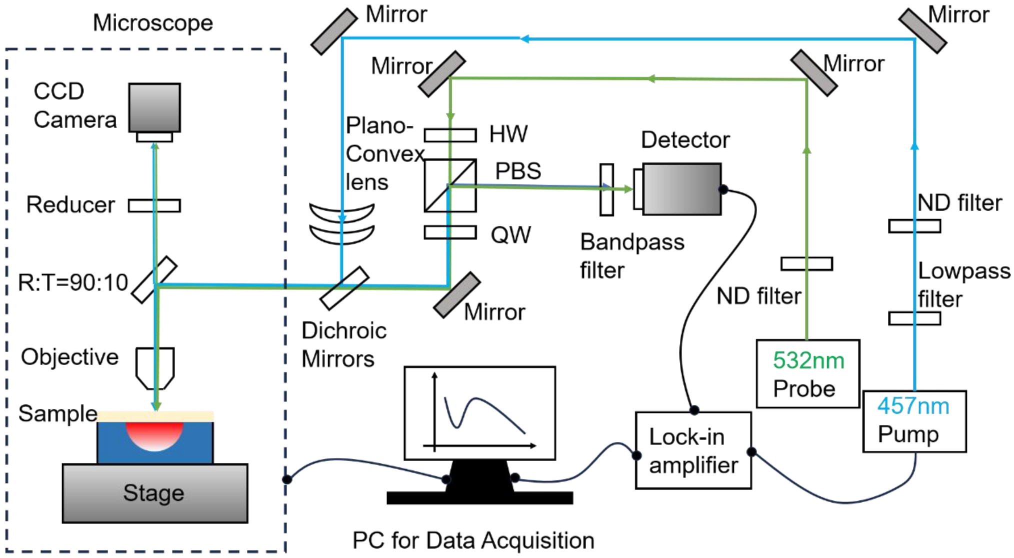

Figure S17. Schematic diagram of the FDTR test principle.

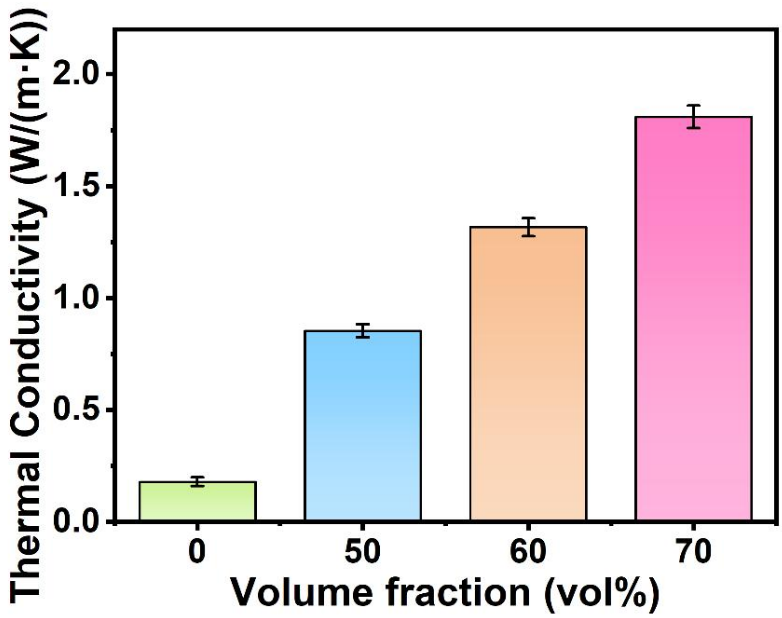

Figure S18. Thermal conductivity of thermal gels with different filler contents.

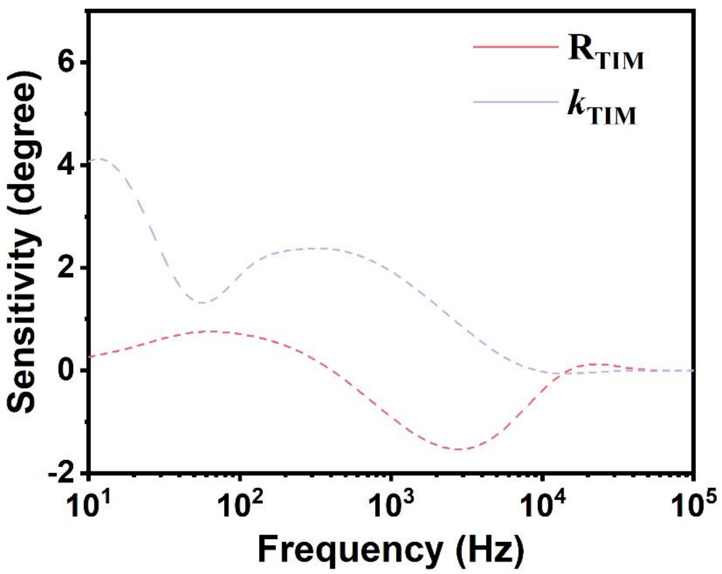

Figure S19. The sensitivity analysis of the FDTR test of commercial TIM.

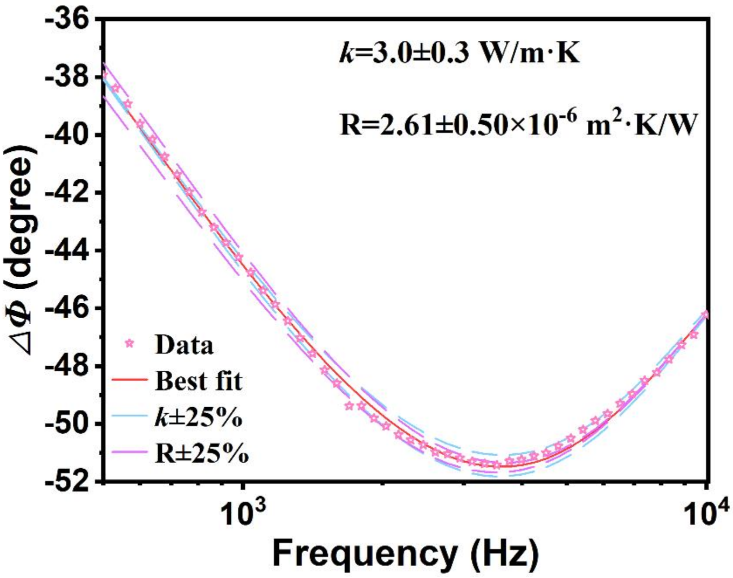

Figure S20. Interface thermal resistance tested by FDTR for commercial TIM.